X-ray speckle-based dark-field imaging of water transport in porous ceramics

Somayeh Saghamanesh[1], Michele Griffa[2], Robert Zboray[1]

[1] Center for X-ray Analytics, Swiss Federal Laboratories for Materials Science and Technology (Empa), 8600 Dübendorf, Switzerland, e-mails: somayeh.saghamanesh@empa.ch; robert.zboray@empa.ch

[2] Concrete and Asphalt Laboratory, Swiss Federal Laboratories for Materials Science and Technology (Empa), 8600 Dübendorf, Switzerland, e-mail: Michele.Griffa@empa.ch

Abstract

The evaluation of liquid transport through porous ceramics are of high importance in numerous applications of these materials, ranging from chemical and physical filters to biomaterials. We present a proof-of-concept of the capability of speckle-based X-ray dark-field imaging (XDFI) for studying the water transport through porous materials with high sensitivity and sub-pixel resolution in a laboratory. Speckle-based imaging (SBI) takes advantage of a simple and flexible setup, with only an additional and inexpensive textured mask, to provide complementary multi-contrast images. Porous ceramic samples with different pore size ranges were imaged in dry and different pure water-saturated states, via an X-ray speckle-tracking setup. The retrieved dark-field images revealed a high sensitivity to (1) the pore size range and to (2) the local water saturation degree. Independently of the pore size range, the dark-field signal decreased upon water saturation. Compared with previously reported laboratory-scale XDFI results for water transport through porous materials, the speckle-tracking approach allows achieving higher temporal and spatial resolutions, thus broadening the range of (water) transport processes which can be investigated without using any contrast agent.

Keywords: porous materials, porous ceramics, water transport, X-ray phase-contrast imaging, dark-field imaging, X-ray speckle-based imaging

1 Introduction

The transport of water (pure or containing ions and other compounds) through most porous materials affects their properties, eventually leading to corrosion, crystal growth, and consequent deformation or even cracking [1]. Porous ceramics have many applications, e.g., as filters for removing chemicals from an environment or as bioactive materials for bone regeneration [2–6]. Therefore, an assessment of the liquid transport properties of porous ceramics is typically needed to characterize its durability and performance [7].

Common methods for such characterization are neutron imaging, nuclear magnetic resonance (NMR) spectroscopy and imaging, and X-ray imaging [1]. The latter is more accessible and allows achieving higher spatial resolution for the same specimen size. Conventional X-ray imaging has been widely used in the laboratory or at synchrotron facilities for studying water transport and pore size distribution in porous materials [8–10]. In this method, a highly-attenuating contrast material (e.g. salt, potassium iodide, lead nitrate) is usually added to the water in order to increase the contrast between pores and the material. However, this is not desired in experiments where the added contrast agent could be adsorbed or react with the porous material or alter fluid properties [11]. Moreover, in standard X-ray imaging and tomography, the pores' size should be above the image resolution, in order to be detected [10,12]. Therefore, the standard image contrast mechanism based on X-ray attenuation, with no contrast agent, has lower sensitivity to local water content changes for most porous materials of practical interest [13]. X-ray phase contrast (XPCI) and dark-field (XDFCI) imaging have been suggested to provide much higher sensitivity to small electron density changes due to water transport [11,12]. These techniques enable to retrieve the refraction and (ultra-)small angle scattering (USAXS, also called dark-field) components of the transmitted X-ray beam, which are much more influenced by local water content changes [14]. The dark-field signal is indeed produced due to the photon scattering from structures at sub-pixel length scales [15].

Yang et al. reported on an X-ray dark-field imaging based on grating interferometry (GI) for tracking water transport in mortar samples [11]. GI relies on advanced phase and absorption gratings, which reduce the overall detected photons, resulting in very long measurement times [16]. Yang et al. [12] obviated the need for an absorbing grating by taking advantage of the high brilliance of synchrotron radiation and a high-resolution detector. However, synchrotron X-ray beams are not available for routine NDT experiments. Furthermore, the complexity of the grating fabrication makes it expensive and difficult to achieve a large field of view for the investigated sample. Finally, GI requires a phase-scanning procedure which may not satisfy the temporal resolution needed for imaging of fast dynamic processes [17–19].

https://doi.org/10.58286/26597

Among demonstrated X-ray phase-sensitive techniques is the speckle-based imaging (SBI), proposed by several investigators [20–22], which enables multi-modal imaging of a sample by tracking near-field speckles created from a diffuser. SBI takes advantage of a simple and flexible setup, with only an additional and inexpensive textured mask, e.g., a sandpaper sheet, positioned between the source and detector (see Fig. 1). This diffuser modulates the intensity and phase of the X-ray wave fronts in the near-field region [23], making it possible to retrieve three image types stemming from three distinct contrast mechanisms: the absorption, the differential phase, and the dark-field contrast images. They can be retrieved from the same raw images acquired at the same time through appropriate algorithms [14,24,25]. This technique provides the phase-sensitivity at all directions also in a single-shot mode. Another advantage of SBI is its independence of the X-ray beam's temporal coherence and its low spatial coherence requirement [26,27].

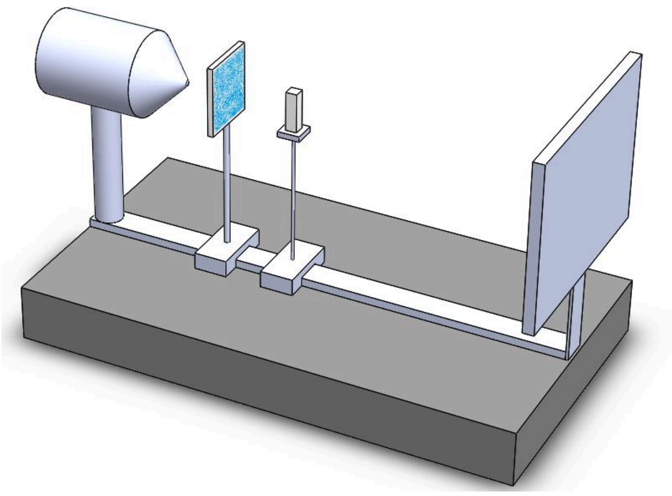

Figure 1: A Schematic of the experimental setup for single-shot X-ray speckle-based imaging.

In this study, we utilize a laboratory implementation of SBI to visualize the changes in pure water saturation degree in porous ceramics with well controlled porosity and pore size ranges. Compared to the propagation-based XPCI [13], SBI enables to retrieve also the dark-field contrast images with almost the same simplicity, photon flux efficiency, and time frame. Moreover, unlike the same multi-contrast imaging realized by GI and reported in previous works [11,12,28], the SBI technique uses only two single images to track the phase-shift and (ultra-)small scattering signals [14]. This is very important from the NDT point of view. It implies a facilitated, inexpensive, and accelerated dynamic imaging and tomography acquisition implementable with laboratory sources. In the following, the implementation of the experiments and analysis is described. In section 3, the results are presented and discussed. A conclusion on the perspectives is contained in section 4.

2 Materials and Methods

Two prismatic porous ceramics samples (alumina and fused silica, DP82/81 and DP215, manufactured by HP Technical Ceramics, UK, for filtration applications) with different pore size ranges (0.3-2 µm and 10-20 µm, respectively) were assessed by our imaging setup. The samples were about 4 mm^2 in the base cross-section and 2 cm high. Before the experiment, they were wrapped by a nylon sheet on all sides except the bottom, intended to be in contact with water, in order to avoid its evaporation from the sides.

The X-ray speckle-tracking setup included a Hamamatsu (L10801) X-ray micro-focus tube operated at 70 kVp and 120 µA. A Gadox scintillator coupled with a CCD camera through fibre optic bundles was used as the detector with a matrix size of 2016 × 1344 and an effective pixel size of 18 µm. The detector was placed at 257 mm downstream the source. The sample was positioned at 55 mm from the source. A sandpaper sheet with an average grain size of 18 µm was placed along the tube's optical axis, 25 mm upstream the sample. The effective pixel size was 3.86 µm. The experiment was performed with both one and a stack of four sandpapers to check the speckle visibility.

As the reference, one radiograph was acquired only with the diffuser in place. The other radiograph was acquired with the diffuser and the sample, hanging over a water container. Each sample was first measured in the dry state. Then, it was lowered to bring its open bottom in contact with the (distilled) water and immersed by 3 mm. Radiographs were then acquired over 2 seconds with averaging 5 successive frames to increase the signal-to-noise ratio. Time-lapse imaging was performed during the capillary suction, with a sampling time of 20 s for a total of 11 hours. The averaged radiographs were processed further in MATLAB by a cross-correlation algorithm [14] with a 13 × 13 subset size to obtain attenuation and dark-field images of the samples.

3. Results and Discussion

The pure attenuation and dark-field radiographs retrieved from the single-shot SBI approach are presented at three time points in Fig. 2 for the sample DP215. When comparing the two radiograph types shown there, no pore space texture is visible in the attenuation radiographs (bottom row) in both dry and wet states. This is also observed upon comparing attenuation and dark-field radiographs retrieved for the DP82/81, shown in Fig. 3.

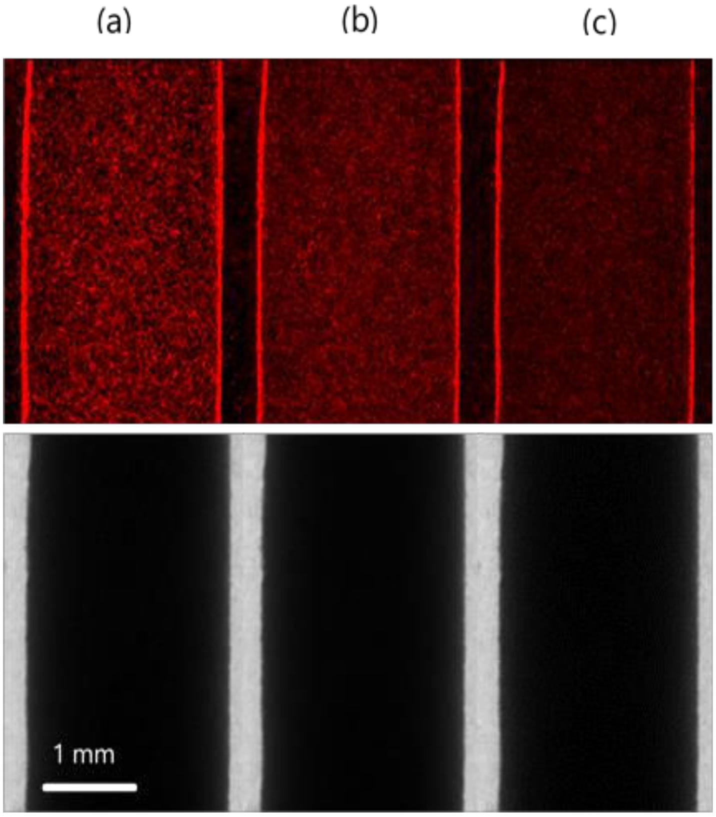

Figure 2: Retrieved dark-field (top) and attenuation (bottom) radiographs of the DP215 ceramics acquired by the single-shot SBI laboratory setup at the time points (a) 0 h, (b) 5.5 h, and (c) 11 h during the gradual water saturation.

However, the dark-field radiographs for both ceramic samples exhibit a clear random texture due to strong (ultra-) small scattering by the porous microstructure (Figs 2, 3-top row). The mean attenuation and dark-field signal (radiograph pixel value) for the samples are reported in Table 1. Unlike the average attenuation signal, which did not mirror any change in the water saturation degree, the average dark-field signal decreased as the water saturation degree increased. This resulted from gradually fading the (ultra-)small angle scattering, and then diffusion, of X-rays upon interaction with the pores partially/fully filled with water [3]. The results with a stack of sandpapers showed a lower speckle visibility, which could be as a result of additional refraction and diffusion between the multiple sandpaper sheets. Since the sandpaper sheets could not be stacked together with zero distance between them, such an inter-space enhanced the photon multiple scattering events. We believe this could increase the speckle blur, and then, decrease the overall visibility, instead of increasing it due to higher attenuation of the speckles.

Generally speaking, the sample with higher pore size range showed stronger dark-field signal than the smaller-pore-size sample. As such, decreasing the dark-field contrast during the gradual water saturation was more pronounced in the former sample than in the latter. Although unsaturated water transport through porous materials depends on many features additional to pore size range, e.g., pore size distribution in the given range, pore size spatial heterogeneity, the presence of cracks as special pores, temperature, and materials properties, the overall sensitivity of X-ray dark-field images to changes in the local water saturation degree can empower the characterization of unsaturated water (or, more generally, liquid) transport through porous materials. The value of such images is especially enhanced if obtained by the more easily implementable and more time-resolved SBI approach. Such value will be strengthened with further understanding of the relationships between pore size range/ distribution and SBI system parameters, speckle characteristic length, and noise reduction, not only for radiographic but also tomographic images.

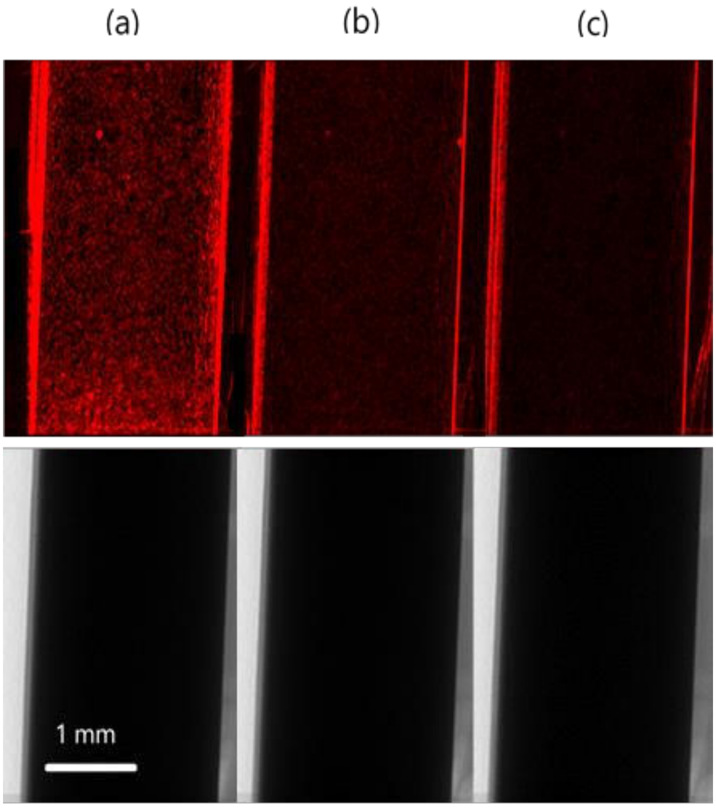

Figure 3: Retrieved dark-field (top) and attenuation (bottom) radiographs of the DP82/81 ceramic sample by the single-shot SBI laboratory setup at the time points (a) 0 h, (b) 5.5 h, and (c) 11 h during the gradual water saturation.

Table 1. Mean attenuation and dark-field signals (pixel values) retrieved at different time points during the gradual water saturation.

Contrast mechanism	Dark-field mean pixel value (a.u.)			Attenuation mean pixel value (a.u.)		
Time (h) / Sample	0	5.5	11	0	5.5	11
DP512	1.94	1.80	1.62	0.222	0.222	0.210
DP82/81	0.82	0.78	0.70	0.090	0.089	0.088

3 Conclusion

This study provides a proof-of-concept for the feasibility of using multi-modal X-ray speckle-based imaging for characterizing (unsaturated) liquid transport through porous materials, without the need of any contrast agents but simply exploiting their inherent microstructural heterogeneity. This technique is simple and fast to set up with a conventional laboratory X-ray source. Furthermore, it doesn't need any long lasting measurement protocol with additional X-ray optics elements, as in X-ray grating interferometry. Thus, it allows achieving higher temporal resolution and it is insensitive to mechanical instabilities, which makes it very suitable for tomography purposes. All these advantages suggests SBI as an inexpensive and easily implementable method for NDT inspections and characterizations.

Acknowledgements

We acknowledge financial support to S. S by the EMPAPOSTDOCS-II programme planned by the European Union's Horizon 2020 research and innovation program under the Marie Skłodowska-Curie grant agreement number 754364. We are grateful to Alexander Flisch for setting up a mechanical arm holder for our experiments.

References

[1] C. Hall, Water sorptivity of mortars and concretes: a review, Mag. Concr. Res. **41**(147) (1989) 51–61.

[2] F. A. Hussain, J. Zamora, I. M. Ferrer, M. Kinyua, and J. M. Velázquez, Adsorption of crude oil from crude oil-water emulsion by mesoporous hafnium oxide ceramics, Environ. Sci. Water Res. Technol. **6**(8) (2020) 2035–2042.

[3] M. Arango-Ospina, Q. Nawaza, and A. R. Boccaccini, Silicate-Based Nanoceramics in Regenerative Medicine, in: V. Guarino, M. Iafisco, and S. Spriano, Nanostructured Biomaterials for Regenerative Medicine, Elsevier Ltd., Erlangen, 2019, pp. 255-273.

[4] C. Wang, Y. Xue, K. Lin, J. Lu, J. Chang, and J. Sun, The enhancement of bone regeneration by a combination of osteoconductivity and osteostimulation using β-CaSiO3/β-Ca 3(PO4)2 composite bioceramics, Acta Biomater. **8**(1) (2012) 350–360.

[5] S. Xu, K. Lin, Z. Wang, J. Chang, L. Wang, J. Lu, and C. Ning, Reconstruction of calvarial defect of rabbits using porous calcium silicate bioactive ceramics, Biomaterials **29**(17) (2008) 2588–2596.

[6] C. Wu and J. Chang, A review of bioactive silicate ceramics, Biomed. Mater. **8**(3) (2013).

[7] A. Khalil, F. Schäfer, N. Postulka, M. Stanzel, M. Biesalski, and A. Andrieu-Brunsen, Wettability-defined droplet imbibition in ceramic mesopores, Nanoscale **12**(47) (2020) 24228–24236.

[8.] N. Shokri, P. Lehmann, and D. Or, Critical evaluation of enhancement factors for vapor transport through unsaturated porous media, Water Resour. Res. **45**(10) (2009) 1–9.

[9] N. Shokri and M. Sahimi, Structure of drying fronts in three-dimensional porous media, Phys. Rev. E - Stat. Nonlinear, Soft Matter Phys. **85**(6) (2012) 1–8.

[10] M. A. Boone, T. De Kock, T. Bultreys, G. De Schutter, P. Vontobel, L. Van Hoorebeke, and V. Cnudde, 3D mapping of water in oolithic limestone at atmospheric and vacuum saturation using X-ray micro-CT differential imaging, Mater. Charact. **97** (2014) 150–160.

[11] F. Yang, F. Prade, M. Griffa, I. Jerjen, C. Di Bella, J. Herzen, A. Sarapata, F. Pfeiffer, and P. Lura, Dark-field X-ray imaging of unsaturated water transport in porous materials, Appl. Phys. Lett. **105**(15) (2014) 1–5.

[12] F. Yang, M. Griffa, A. Hipp, H. Derluyn, P. Moonen, R. Kaufmann, M. N. Boone, F. Beckmann, and P. Lura, Advancing the visualization of pure water transport in porous materials by fast, talbot interferometry-based multi-contrast x-ray micro-tomography, Dev. X-Ray Tomogr. X **9967**(October 2016), 99670L.

[13] F. Yang, M. Griffa, A. Bonnin, R. Mokso, C. Di Bella, B. Münch, R. Kaufmann, and P. Lura, Visualization of water drying in porous materials by X-ray phase contrast imaging, J. Microsc. **261**(1) (2016) 88–104.

[14] M. C. Zdora, State of the Art of X-ray Speckle-Based Phase-Contrast and Dark-Field Imaging, J. Imaging **4**(5) (2018).

[15] M. Ando, N. Sunaguchi, D. Shimao, A. Pan, T. Yuasa, K. Mori, Y. Suzuki, G. Jin, J. K. Kim, J. H. Lim, S. J. Seo, S. Ichihara, N. Ohura, and R. Gupta, "Dark-Field Imaging: Recent developments and potential clinical applications," Phys. Medica **32**(12) (2016) 1801–1812.

[16] S. Saghamanesh, S. M. Aghamiri, A. Kamali-Asl, and W. Yashiro, Photon detection efficiency of laboratory-based x-ray phase contrast imaging techniques for mammography: A Monte Carlo study, Phys. Med. Biol. **62**(18) (2017) 7394–7406.

[17] A. Kaestner, B. Münch, and L. Butler, Spatiotemporal computed tomography of dynamic processes, Opt. Eng. **50**(12) (2011) 123201.

[18] J. D. Schaap, P. Lehmann, A. Kaestner, P. Vontobel, R. Hassanein, G. Frei, G. H. de Rooij, E. Lehmann, and H. Flühler, Measuring the effect of structural connectivity on the water dynamics in heterogeneous porous media using speedy neutron tomography, Adv. Water Resour. **31**(9) (2008) 1233–1241.

[19] F. Prade, K. Fischer, D. Heinz, P. Meyer, J. Mohr, and F. Pfeiffer, Time resolved X-ray Dark-Field Tomography Revealing Water Transport in a Fresh Cement Sample, Sci. Rep. **6**(June) (2016) 1–7.

[20] S. Bérujon, E. Ziegler, R. Cerbino, and L. Peverini, Two-dimensional x-ray beam phase sensing, Phys. Rev. Lett. **108**(15) (2012) 1–5.

[21] K. S. Morgan, D. M. Paganin, and K. K. W. Siu, X-ray phase imaging with a paper analyzer, Appl. Phys. Lett. **100**(12), (2012).

[22] S. Berujon, H. Wang, and K. Sawhney, X-ray multimodal imaging using a random-phase object, Phys. Rev. A - At. Mol. Opt. Phys. **86**(6) (2012) 1–9.

[23] R. Cerbino, L. Peverini, M. A. C. Potenza, A. Robert, P. Bösecke, and M. Giglio, X-ray-scattering information obtained from near-field speckle, Nat. Phys. **4**(3) (2008) 238–243.

[24] K. M. Pavlov, H. (Thomas) Li, D. M. Paganin, S. Berujon, H. Rougé-Labriet, and E. Brun, Single-Shot X-Ray Speckle-Based Imaging of a Single-Material Object, Phys. Rev. Appl. **13**(5) (2020).

[25] D. M. Paganin, H. Labriet, E. Brun, and S. Berujon, Single-image geometric-flow x-ray speckle tracking, Phys. Rev. A **98**(5), (2018).

[26] I. Zanette, T. Zhou, A. Burvall, U. Lundström, D. H. Larsson, M. Zdora, P. Thibault, F. Pfeiffer, and H. M. Hertz, Speckle-based x-ray phase-contrast and dark-field imaging with a laboratory source, Phys. Rev. Lett. **112**(25) (2014) 1–5.

[27] S. Saghamanesh and R. Zboray, Virtual speckle-based X-ray phase-contrast and dark-field imaging with digital phantoms, Opt. Express **29**(25) (2021) 41703.

[28] V. Revol, I. Jerjen, C. Kottler, P. Schtz, R. Kaufmann, T. Lthi, U. Sennhauser, U. Straumann, and C. Urban, Sub-pixel porosity revealed by x-ray scatter dark field imaging, J. Appl. Phys. **110**(4) (2011).